Myeloma-Induced Alloreactive T Cells Arising in Myeloma-Infiltrated Bones Include Double-Positive $CD8^+CD4^+$ T Cells: Evidence from Myeloma-Bearing Mouse Model

Lisa M. Freeman,* Alfred Lam,† Eugene Petcu,† Robert Smith,† Ali Salajegheh,† Peter Diamond,‡ Andrew Zannettino,‡ Andreas Evdokiou,§,¶ John Luff,‖ Pooi-Fong Wong,# Dalia Khalil,* Nigel Waterhouse,* Frank Vari,‖ Alison M. Rice,*, Laurence Catley,* Derek N. J. Hart,†† and Slavica Vuckovic*,****

The graft-versus-myeloma (GVM) effect represents a powerful form of immune attack exerted by alloreactive T cells against multiple myeloma cells, which leads to clinical responses in multiple myeloma transplant recipients. Whether myeloma cells are themselves able to induce alloreactive T cells capable of the GVM effect is not defined. Using adoptive transfer of T naive cells into myeloma-bearing mice (established by transplantation of human RPMI8226-TGL myeloma cells into $CD122^+$ cell-depleted NOD/SCID hosts), we found that myeloma cells induced alloreactive T cells that suppressed myeloma growth and prolonged survival of T cell recipients. Myeloma-induced alloreactive T cells arising in the myeloma-infiltrated bones exerted cytotoxic activity against resident myeloma cells, but limited activity against control myeloma cells obtained from myeloma-bearing mice that did not receive T naive cells. These myeloma-induced alloreactive T cells were derived through multiple $CD8^+$ T cell divisions and enriched in double-positive (DP) T cells coexpressing the CD8αα and CD4 coreceptors. MHC class I expression on myeloma cells and contact with T cells were required for $CD8^+$ T cell divisions and DP-T cell development. DP-T cells present in myeloma-infiltrated bones contained a higher proportion of cells expressing cytotoxic mediators IFN-γ and/or perforin compared with single-positive $CD8^+$ T cells, acquired the capacity to degranulate as measured by CD107 expression, and contributed to an elevated perforin level seen in the myeloma-infiltrated bones. These observations suggest that myeloma-induced alloreactive T cells arising in myeloma-infiltrated bones are enriched with DP-T cells equipped with cytotoxic effector functions that are likely to be involved in the GVM effect. *The Journal of Immunology*, **2011, 187: 3987–3996.**

In multiple myeloma (MM) patients, donor leukocyte infusion (DLI) after allogeneic hematopoietic stem cell transplantation as prophylaxis for myeloma relapse or as relapse treatment can provide effective therapy, achieving clinical responses in 40–67% of patients (1). The curative effect of DLI is believed to be due to donor alloreactive T cells that exert an immune attack against myeloma cells, which is clinically defined as a graft-versus-myeloma (GVM) effect (2–4). Key features of the GVM responses, including the priming of alloreactive T cells by host and/or tumor cells, localization, phenotype, and functional properties of alloreactive T cells, cannot be examined in the clinical setting. An experimental approach based on adoptive transfer of allogeneic T cells into myeloma-bearing mice offers a practical opportunity to overcome clinical limitations. Indeed, adoptive transfer of allogeneic PBMCs or T cells into myeloma-bearing $RAG2^{-/-}\gamma c^{-/-}$ mice leads to myeloma suppression (5). However, the alloreactive T cells that cause the GVM effect, in particular direct proof for their capacity to eliminate myeloma cells, are yet to be defined.

Several related hypotheses can be proposed to explain how alloreactive T cells develop and contribute to GVM responses. It is plausible that alloreactive T cells might accumulate in the myeloma target organ, the myeloma-infiltrated bones, and need to be programmed within the myeloma-infiltrated bones to undergo proliferation and differentiation into T effector cells capable of myeloma cell elimination. It is a widely accepted view that tumor cells are inefficient at inducing T cell responses, for two reasons, as follows: 1) they are not professional APCs because of loss of function (e.g., decreased adhesion molecules) and/or gain of (dys) function (e.g., secretion of immunosuppressive cytokines) (6), and 2) in many cases, the tumor is not located in lymphoid organs, which inherently support T cell responses (7). However, if tumor cells or nonprofessional APCs reach lymphoid organs, measurable cytotoxic T cell responses can be induced (8). Given that myeloma cells infiltrate bone marrow, a primary lymphoid organ for T cell responses (9, 10), it is possible that myeloma cells interacting with

*Mater Medical Research Institute, Queensland 4101, Australia; †School of Medicine, Griffith University, Queensland 4222, Australia; ‡Centre for Cancer Biology, Institute for Medical and Veterinary Science and Robinson Institute, University of Adelaide, South Australia 5000, Australia; §University of Adelaide, South Australia 5000, Australia; ¶Hanson Institute, South Australia 5000, Australia; ‖Queensland Institute of Medical Research, Queensland 4029, Australia; #Faculty of Medicine, University of Malaya, 50603 Kuala Lumpur, Malaysia; **University of Queensland, Queensland 4072, Australia; and ††Australian and New Zealand Army Corps Research Institute, New South Wales 2139, Australia

Received for publication April 26, 2011. Accepted for publication August 9, 2011.

This work was supported by a Leukaemia Research Fund U.K. International fellowship (to L.M.F.), the National Health and Medical Research Council and Leukaemia Foundation Australia (to S.V. and L.C.), the Cancer Council Queensland (to D.N.J.H.), an Australian Endeavour Award (to P.-F.W.), and a Queensland Government Smart Futures fellowship (to A.M.R.).

Address correspondence and reprint requests to Dr. Slavica Vuckovic, Mater Medical Research Institute, Aubigny Place, Raymond Terrace, South Brisbane, QLD 4101, Australia. E-mail address: svuckovic@mmri.mater.org.au

The online version of this article contains supplemental material.

Abbreviations used in this article: 7-AAD, 7-aminoactinomycin D; DLI, donor leukocyte infusion; DP, double-positive; GVM, graft-versus-myeloma; hu, human; Luc, luciferase; m, mouse; MM, multiple myeloma; Sp, spleen; SP, single-positive; T_{CM}, T central memory; T_N, T naive.

donor T cells reaching myeloma-infiltrated bones following DLI would be able to induce alloreactive T cells capable of exerting an antimyeloma effect.

We assessed myeloma growth and associated alloreactive T cell responses using adoptive transfer of human T naive (T_N) cells into myeloma-bearing mice established by transplantation of GFP and luciferase (Luc)-expressing human RPMI8226 myeloma cells [RPMI8226-TGL cells (11)] into $CD122^+$ cell-depleted NOD/SCID hosts. In these myeloma-bearing mice, myeloma involves multiple bones, but not soft tissues, with secretion of λ-chain and the development of bone lesions that mimic the clinical features of MM (12, 13). Also, in these myeloma-bearing mice, myeloma cells are the only cells expressing human MHC required for interactions with adoptively transferred T_N cells.

Our data suggest that myeloma-induced alloreactive T cells lead to transient myeloma suppression in myeloma-bearing mice. Myeloma-induced alloreactive T cells arising in the myeloma-infiltrated bones exert cytotoxic activity against resident myeloma cells and involve nonconventional double-positive (DP) $CD8^+$ $CD4^+$ T cells with cytotoxic effector functions that are likely to be involved in the GVM effect.

Materials and Methods

Mice

Female NOD/SCID mice were housed at the animal facility in the Mater Medical Research Institute or the Queensland Institute of Medical Research. Experimental work involving animals was approved by the University of Queensland and the Queensland Institute of Medical Research Animal Ethics Committees. Mice were sublethally irradiated (325 cGy, [^{137}Cs] source), treated or untreated with anti-mouse CD122 mAb (BioXCell, West Lebanon, NH; 1 mg/mouse, i.p. injection, hereafter referred to as $CD122^+$ cell-depleted or $CD122^+$ cell-replete hosts, respectively), and then transplanted with human RPMI8226, RPMI8226-TGL, or U266 myeloma cells.

Myeloma cell lines

The human myeloma cell lines, RPMI8226 and U266, were purchased from the American Type Culture Collection (NSW, Australia). The RPMI8226-TGL cell line was produced by transduction of RPMI8226 myeloma cells with the NES–TGL construct expressing GFP and firefly Luc (11). All myeloma cell lines were maintained in DMEM supplemented with 4.5 g/l D-glucose, 10% FCS, 100 U/ml penicillin, 100 mg/ml streptomycin, 2 mM L-glutamine, 1 mM sodium pyruvate, and 10 mM HEPES.

Preparation of human T_N cells

Collection of aphaeresis products from healthy donors was approved by the Mater Adult Hospital Human Ethics Committee. From an aphaeresis product, T_N cells were isolated by magnetic depletion of CD11c, CD16, CD14, CD19, CD20, CD34, CD56, HLA-DR, Gly-A, CD45RO-stained cells (1.3-4.2 × 10^8 $CD3^+CD45RA^+$ cells; purity >95%, CliniMACS DEPL2.1; Miltenyi Biotec, Bergisch Gladbach, Germany). All mAb were purchased from Coulter Immunotech (Gladesville, NSW, Australia). A cohort of myeloma-bearing mice (established by transplantation of RPMI8226-TGL myeloma cells into $CD122^+$ cell-depleted hosts) at day 8–12 after myeloma cell transplantation was split into two groups, as follows: 1) control mice who did not receive T_N cells and 2) T cell recipient mice who received unlabeled or CFSE-labeled T_N cells (Molecular Probes, Eugene, OR; 3–4 × 10^7 T_N cells/mouse, i.v. injection). During the course of the experiments, T cell recipient mice did not show any evidence of weight loss or diarrhea indicative of a xenogeneic graft-versus-host response. We sought to include another group of control $CD122^+$ cell-depleted mice receiving T_N cells in the absence of MM, but this was not practicable because of extremely low or absent T_N cell engraftment in these animals (14). GFP^+ myeloma cells and mouse $CD45^+$ cells were sorted from cell suspensions prepared from pooled bones (femur, tibia, pelvic bones, lumbar, and thoracic vertebrae) harvested from myeloma-bearing mice. Unlabeled and CFSE-labeled T_N cells were maintained with sorted GFP^+ myeloma cells or mouse $CD45^+$ cells in coculture or Transwell assays for 5 d. In some coculture experiments, blocking anti-MHC class I (HLA-ABC, W6/32; eBioscience, NSW, Australia), anti-MHC class II (HLA-DR, DP, DQ; BD Biosciences, NSW, Australia), or control IgG mAb were added to the culture medium.

Histopathological and immunohistochemical analysis

Bone and soft tissues were harvested at the end stage of disease, fixed in formalin, and embedded in paraffin. Sections were cut and stained with H&E. For immunohistochemical analysis, sections were stained using the Novolink Polymer Detection System (Novocastra Laboratories, Newcastle Upon Tyne, U.K.) in a Labvision 360 Autostainer (Lab Vision, Freemont, CA).

Microcomputer tomography analysis

Hind limbs, lumbar vertebrae, and skull from myeloma-bearing mice at end stage of disease and control $CD122^+$ cell-depleted mice that had not received myeloma cells were harvested in 70% ethanol and scanned by 18-μm resolution using the SkyScan-1076 micro-CT scanner. Images were generated using Cone-Beam reconstruction via CT analyzer and three-dimensional visualization software programs (SkyScan, Kontich, Belgium).

Flow cytometric analysis

Cell suspensions were prepared from femur, tibia, pelvic bones, lumbar vertebrae, thoracic vertebrae, and spleen (Sp) harvested from individual T cell recipients at day 6–10 after adoptive T_N cell transfer and analyzed by flow cytometry (FACSCalibur, LSRII BD). To detect T cell proliferation ($CD8^+$ T and $CD8^-$ T subsets), CFSE-labeled $CD3^+$ T_N cells were stained with mouse (m)CD45-PerCP/human (hu)CD3-allophycocyanin/huCD8-PE mAb. To define the phenotype of $CD3^+$ T cells, cells were stained with mCD45PerCP/huCD45 allophycocyanin-H7/CD3-allophycocyanin/huCD8-PECy7/huCD4-PE combined with huCD45RO-FITC or huCD62L-FITC mAb. To define expression of CD8αα and CD8β on T cells, cells were stained with mCD45PerCP/huCD45 allophycocyanin-H7/CD3-allophycocyanin/huCD8-PECy7/huCD4-FITC and huCD8αβ-PE. To define activated $CD3^+$ T cells, cells were stained with huCD3PerCP/huCD8-PECy7/huCD25-allophycocyanin/huCD127-PE/huCD4-FITC mAb. For intracellular cytokines, perforin expression, and degranulation, cells were stained with huCD3PerCP/huCD8-PECy7/huCD4-FITC/huCD107a-allophycocyanin mAb, fixed/permeabilized, and stained with huIFN-γ–Alexa700, huPerforin-PE, huIL-2–PE, huIL-5–PE, and huIL-13–PE mAb. To define the phenotype of GFP^+ myeloma cells, cells were stained with huCD38-PE, huClass I-PE, huCD56-PE, and huHLA-DR–allophycocyanin mAb. To measure apoptotic myeloma cells, cells were stained with annexin V and 7-aminoactinomycin D (7-AAD). All mAb were purchased from BD Biosciences (NSW, Australia), unless otherwise indicated.

Bioluminescent imaging

Whole-body bioluminescent imaging was performed using an IVIS 100 bioluminescence optical imaging system (Xenogen, Alameda, CA). Prior to imaging, each mouse received a s.c. injection of luciferin (1 μg/mouse; Biolab Australia, Clayton, VIC, Australia). Optical images were displayed and analyzed using the Igor and IVIS Living Image software packages (WaveMetrics, Lake Oswego, OR; Xenogen).

In vitro Luc assay

Tissue lysates were prepared from bones and visceral organs harvested from myeloma-bearing mice at days 1, 7, 14, and 34 (end stage of disease) after myeloma cell injection using lysis buffer (Luciferase Assay Kit; Promega, Madison, WI). Luminescence produced by myeloma cells was measured using 10-s measurement read time (FLUOstar OPTIMA; BMG Labtech, VIC, Australia) and standardized as relative light units/mg protein (BCA Protein Assay Kit; Pierce, Rockford, IL).

ELISA for human λ-chain and perforin

The λ-chain concentration was analyzed in serum samples using the human λ ELISA quantification kit (Bethyl Laboratories, Montgomery, TX), according to the manufacturer's protocol. Cells from two femurs, two tibias, and Sp from individual T cell recipient mice were harvested in washing buffer (2 ml HBSS supplemented with 20% FCS). After cell removal, perforin was assessed in the washing buffer using the human perforin ELISA kit (Abcam, Cambridge, U.K.), according to the manufacturer's protocol. Absorbance was measured using a microplate reader (iMark; Bio-Rad, NSW, Australia).

[^{51}Cr] release assays

Cell suspensions were prepared from pooled myeloma-infiltrated bones (femur, tibia, pelvic bones, lumbar vertebrae, thoracic vertebrae) and uninvolved Sp of individual T cell recipient mice and from pooled myeloma-

infiltrated bones of control myeloma-bearing mice that did not receive T_N cells. To isolate myeloma cells from myeloma-infiltrated bones of T cell recipient and control myeloma-bearing mice (referred to as resident and control myeloma cells, respectively), cells were stained with huCD38 mAb (Beckman Coulter, NSW, Australia) prior to positive selection (AutoMACS, Posselds; Miltenyi Biotec), and GFP^+CD38^+ myeloma cells were sorted (FACSAria; BD Bioscience; >98% cell purity). To isolate T cells from myeloma-infiltrated bones and uninvolved Sp of individual T cell recipients, cells were stained with huCD2 mAb (Beckman Coulter) prior to positive selection of $CD2^+$ T cells (>85% cell purity; AutoMACS Posselds). Sorted resident and control myeloma cells were ^{51}Cr labeled and incubated with T cells for 4 h (myeloma/T cell ratio 1:25, 1:50); supernatant was collected and counted for released [^{51}Cr] (Wallac liquid scintillation counter, Boston, MA). The specific lysis of myeloma cells was calculated by the following equation: (experimental release − spontaneous release/maximum release − spontaneous release) × 100.

Statistical analysis

Data are presented as mean ± SEM or median ± interquartile range dependent on the normality of data. The *t* test and Mann–Whitney *U* test were used to compare continuous variables between individual mice. Log-rank Mantel–Cox test was used to compare survival curves of T cell recipients and control mice. Differences were considered statistically significant at the 0.05 level. Analysis was performed using GraphPad Prism 5.0 software (San Diego, CA).

Results

Myeloma cells transplanted into $CD122^+$ cell-depleted hosts involve multiple bones and lead to bone lesions

We sought to develop a new myeloma mouse model that mimics typical features of clinical MM such as bone involvement and bone lesions, and ultimately may improve current myeloma mouse models (5, 15). To achieve this, we used experimental approaches based on transplantation of human RPMI8226, RPMI8226-TGL, or U266 myeloma cells into $CD122^+$ cell-depleted and $CD122^+$ cell-replete NOD/SCID hosts.

In $CD122^+$ cell-depleted mice, transplanted RPMI8226 or RPMI8226-TGL myeloma cells expressing CD38, CD56, class I, and λ-chain infiltrated multiple bones, but were rarely found in visceral organs (Fig. 1*A*, 1*B*, Supplemental Table I). These mice had bone lesions detectable in the tibia, lumbar vertebrae, and skull (lesions indicated by arrows; Fig. 1*C*) and did not develop s.c. plasmacytomas, and <3% of animals had extramedullary tumors on autopsy. Serum λ-chain was detectable in all animals, and 95% of mice developed hind limb paralysis with a median survival time of 49 d. Overall, transplantation of RPMI8226 or RPMI8226-TGL myeloma cells into $CD122^+$ cell-depleted as opposed to $CD122^+$ cell-replete hosts led to greater bone involvement and shorter survival time. Transplantation of U266 myeloma cells into $CD122^+$ cell-depleted or $CD122^+$ cell-replete hosts resulted in barely detectable myeloma engraftment by flow cytometry and no disease symptoms within 90 d posttransplantation (Supplemental Table I); therefore, it was not a practicable approach to create a myeloma mouse model using these cells.

Bioluminescence imaging showed a faster rate of myeloma growth in $CD122^+$ cell-depleted than $CD122^+$ cell-replete hosts transplanted with RPMI8226-TGL myeloma cells (Fig. 1*D*, 1*E*). To assess the pattern of organ involvement, which is difficult to accurately predict from optical images, we measured the amount of Luc activity (representative of myeloma mass) present in various bones and visceral organs at days 1, 7, 14, and 34 (end stage of disease) after RPMI8226-TGL myeloma cell transplantation into $CD122^+$ cell-depleted hosts. Bones, rather than visceral organs, were the major site of myeloma growth from day 7 to the end stage of disease (Fig. 1*F*, and data not shown). Initially, myeloma cells infiltrated the femur, tibia, and pelvis bones, and, thereafter, expanded to involve the skull, thoracic vertebrae, and most extensively the lumbar vertebrae (Fig. 1*F*). In sharp contrast to other bones, myeloma cells remained at low levels in the forelimb and ribs until the end stage of disease (Fig. 1*F*). Gradually over time, myeloma cells infiltrated visceral organs, as follows: brain, liver, lung by day 14 postmyeloma cell transplantation, followed by the Sp and kidney at the end stage of disease; but the degree of the visceral organ involvement was far less than the bone involvement (Fig. 1*F*). Together, different measures of myeloma growth suggest that transplantation of myeloma cells (RPMI8226 or RPMI8226-TGL) into $CD122^+$ cell-depleted hosts leads to bone involvement and bone lesions resembling the clinical evolution of MM.

Adoptive transfer of T_N cells into myeloma-bearing mice suppresses myeloma growth and prolongs survival of T cell recipients

Next, we analyzed whether adoptive transfer of human T_N cells into myeloma-bearing mice (established by transplantation of RPMI8226-TGL cells into $CD122^+$ cell-depleted hosts) can suppress myeloma growth and prolong survival of T cell recipients, indicative of a GVM effect, compared with control mice that did not receive T_N cells. In the myeloma-infiltrated bones of T cell recipients, at day 9–10 after adoptive T_N cell transfer, the proportion of GFP^+ myeloma cells tended to be lower and reached significant differences in thoracic vertebrae compared with the myeloma-infiltrated bones of control mice (Fig. 2*A*). Bioluminescent imaging of T cell recipients revealed a delay in myeloma growth compared with control mice, but over time myeloma signals increased, reaching levels similar to that seen in control mice (Fig. 2*B*). Also, in T cell recipients, there was delay in the rise of serum λ (in six of nine mice) compared with control myeloma-bearing mice, but again, over time serum λ increased, reaching levels similar to that seen in control mice (Fig. 2*C*). Myeloma suppression, albeit transient, significantly improved survival of T cell recipients who died within 67 d after myeloma cell injection, whereas control mice died 42 d after myeloma cell injection (median survival 42 versus 32 d; Fig. 2*D*).

T cells from myeloma-infiltrated bones exert cytotoxic activity against resident myeloma cells

We hypothesized that the development of alloreactive T cells capable of myeloma elimination could explain the transient myeloma suppression and prolonged survival observed in T cell recipients. Therefore, we analyzed cytotoxic activity of T cells harvested from myeloma-infiltrated bones and uninvolved Sp against resident and control myeloma cells. Adoptively transferred T_N cells were uniformly distributed throughout MM-infiltrated bones, but were more abundant in uninvolved Sp (Fig. 3*A*). T cells harvested from myeloma-infiltrated bones were more efficient at lysing resident myeloma cells compared with these derived from uninvolved Sp (Fig. 3*B*). Time lapse microscopy showed that resident GFP^+ myeloma cells underwent morphological changes typical for apoptosis after being in contact with T cells derived from myeloma-infiltrated bones (Supplemental Video 1). Interestingly, T cells harvested from myeloma-infiltrated bones or uninvolved Sp showed limited cytotoxic activity against control myeloma cells obtained from myeloma-bearing mice that did not receive T_N cells (Fig. 3*B*). In the myeloma-infiltrated bones of T cell recipients, the proportion of late apoptotic myeloma cells ($7\text{-}AAD^+$ $annexin^+$ cells) tended to be higher and reached significant differences in tibia compared with the myeloma-infiltrated bones of control mice that did not receive T_N cells (Fig. 3*C*). These experiments provide direct proof that

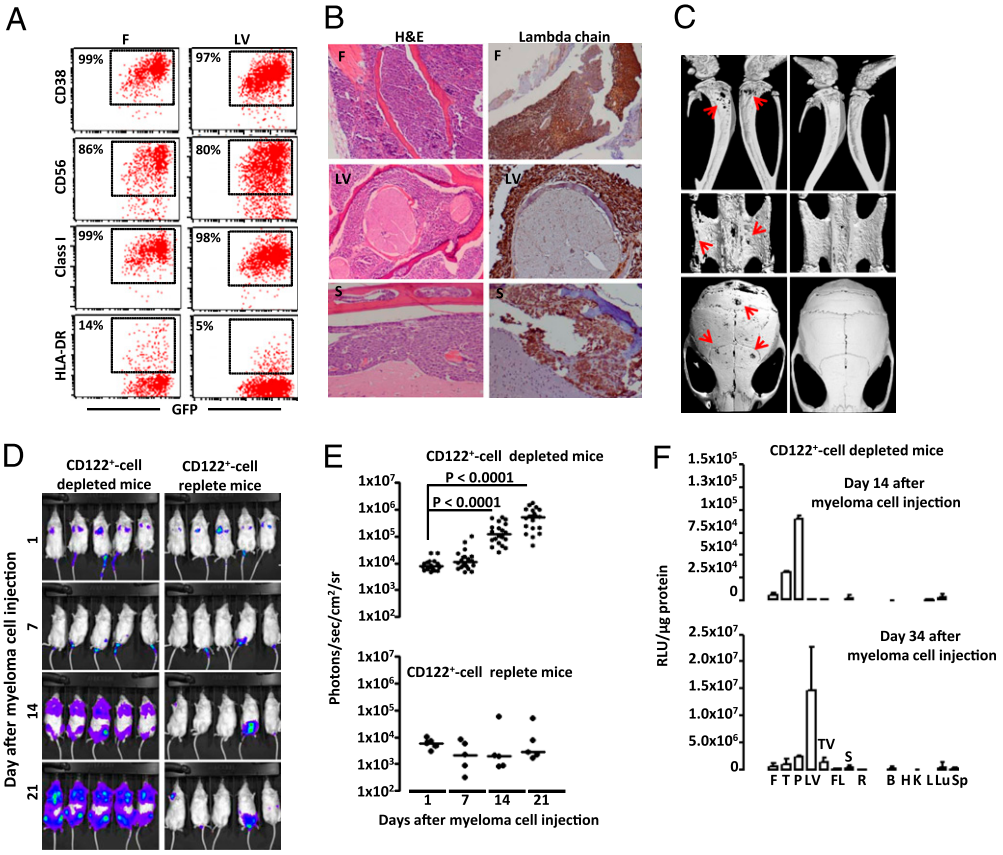

FIGURE 1. Monitoring myeloma growth in CD122$^+$ cell-depleted and CD122$^+$ cell-replete mice. *A*, Flow cytometry analyses of myeloma cells in the femur and lumbar vertebrae of CD122$^+$ cell-depleted mice transplanted with RPMI8226-TGL myeloma cells at end stage disease (percentages represent the proportion of GFP$^+$ myeloma cells outlined by squares expressing indicated Ag). *B*, Histopathological appearance and immunohistochemical detection of λ-chain in the myeloma-infiltrated femur, lumbar vertebrae, and skull of CD122$^+$ cell-depleted mice transplanted with RPMI8226 myeloma cells at end stage disease (H&E, original magnification ×4; λ$^+$ myeloma cells, brown staining, original magnification ×10). *C*, Micro-CT three-dimensional reconstructions of the longitudinal sections of tibia, lumbar vertebrae, and skull of CD122$^+$ cell-depleted mice transplanted with RPMI8226-TGL myeloma cells (at end stage disease; bone lesions indicated by arrows) and control CD122$^+$ cell-depleted mice that were not transplanted with myeloma cells (*left* and *right panels*, respectively). *D*, Consecutive bioluminescence imaging of the CD122$^+$ cell-depleted and CD122$^+$ cell-replete mice transplanted with RPMI8226-TGL myeloma cells (blue is minimal and red is maximal light intensity, exposure time 10 s). *E*, Individual data points of bioluminescent myeloma signal emitted from identical sized images of CD122$^+$ cell-depleted (median, $n = 20$) and CD122$^+$ cell-replete (median, $n = 5$) mice transplanted with RPMI8226-TGL myeloma cell. Mice that had not been transplanted with myeloma cells were used to define the background bioluminescent signal ($<1 \times 10^3$ photon/s/cm^2/sr). *F*, Luc activity of duplicate measurements of each tissue lysate sample prepared from indicated bones and visceral organs of CD122$^+$ cell-depleted mice transplanted with RPMI8226-TGL myeloma cells (median with interquartile range; two mice at each time point). B, brain; F, femur; FL, forelimb; H, heart; K, kidney; L, liver; Lu, lung; LV, lumbar vertebrae; P, pelvic bones; R, ribs; S, skull; Sp, spleen; T, tibia, TV, thoracic vertebrae.

T cells arising in myeloma-infiltrated bones of T cell recipients exert cytotoxic activity against resident myeloma cells.

Myeloma cells prime alloreactive T cells via MHC class I in a contact-dependent manner and induce DP-T cells coexpressing CD8αα and CD4

Next, we analyzed the proliferation and phenotype of alloreactive T cells capable of myeloma elimination and explored the role for myeloma cells in these processes. In both myeloma-infiltrated bones and uninvolved Sp, adoptively transferred CD8$^+$ T cells divided more vigorously than CD8$^-$ T cells (corresponding to CD4$^+$ T cells); therefore, CD8$^+$ T cells became the dominant T cell type representing >63% of total T cells (Fig. 4*A*, *bottom panel*). The nonconventional DP-CD8$^+$CD4$^+$ T cells, which were negligible among the T_N cells at the time of injection, increased in myeloma-infiltrated bones and accounted for 27–38% of total CD3$^+$ T cells, but remained low in uninvolved Sp (13% of total CD3$^+$ T cells) (Fig. 4*B*). Proportions of conventional single-positive (SP)-CD8$^+$CD4$^-$ T cells in the myeloma-infiltrated bones remained similar to that seen among T_N cells at the time of injection, but tended to be increased in the uninvolved Sp (Fig. 4*B*). Thus, nonconventional DP-T cells in myeloma-infiltrated bones, but conventional SP-CD8$^+$ T cells in the uninvolved Sp accounted for the majority of the overall increase in CD8$^+$ T cells seen in T cell recipients (Fig. 4*A*). Both DP-T cells and SP-CD8$^+$ T cells derived from myeloma-infiltrated bones resembled the phenotype of T effector memory (T_{EM}) cells expressing CD45RO and lacking CD62L, CD25, and CD127 surface Ags (Fig. 4*C*). Furthermore, DP-T cells and SP-CD8$^+$ T cells in myeloma-infiltrated bones converted CD8αβ heterodimer (expressed on SP-CD8$^+$ T at the time of injection) to CD8αα homodimer (Fig. 4*C*).

We presumed that in myeloma-bearing mice, myeloma cells expressing human MHC induce CD8$^+$ T cell proliferation and consequently DP-T cells. Therefore, we analyzed the capacity of myeloma cells and mouse CD45$^+$ cells isolated from the same myeloma-infiltrated bones of myeloma-bearing mice to induce CD8$^+$ T cell proliferation and DP-T cells using in vitro culture. Myeloma cells, but not mouse CD45$^+$ cells, were able to induce CD8$^+$ T cell proliferation (Fig. 5*A*, *top panel*). This myeloma-

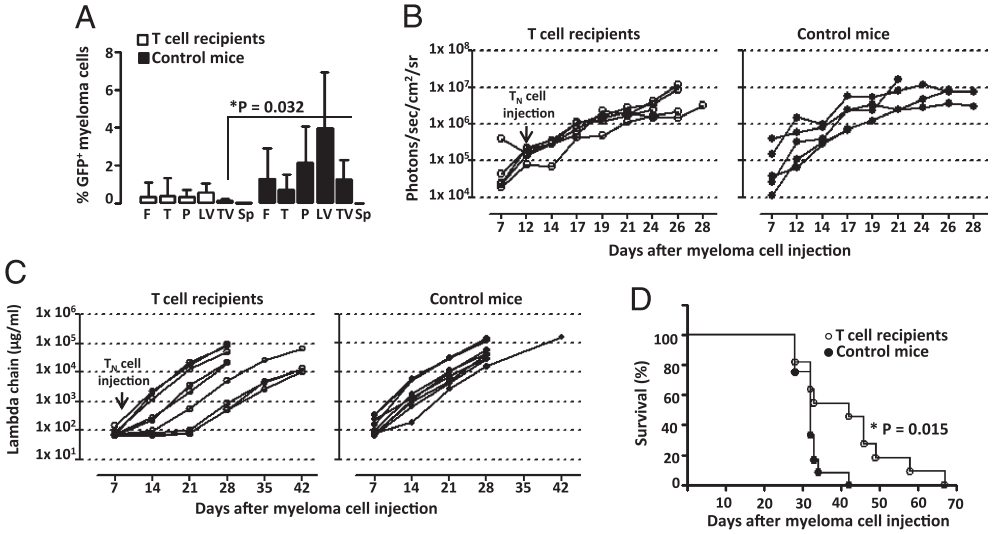

FIGURE 2. Evidence for myeloma suppression in the T cell recipients. Myeloma growth was measured in parallel in T cell recipients (in multiple experiments, mice received T_N cells at day 8–12 after transplantation of RPMI8226-TGL myeloma cells into $CD122^+$ cell-depleted hosts) and control mice (did not receive T_N cells). *A*, Flow cytometry analysis of GFP^+ myeloma cells in myeloma-infiltrated bones and uninvolved Sp of T cell recipients and control mice (at day 9–10 after T_N cells or day 18–19 after myeloma cell injection, bar, mean ± SEM; 4–5 mice/group). *B*, Bioluminescent myeloma signal emitted from identical sized images of the T cell recipients and control mice (5 mice/group). *C*, Serum λ concentration in T cell recipients and control mice (9 mice/group). *D*, Survival of T cell recipient and control mice was monitored over period of 58 d after T_N cell injection and 67 d after the initial myeloma cell injection (11–12 mice/group).

induced $CD8^+$ T cell proliferation was not detected in Transwell experiments in which cell-to-cell contact between myeloma cells and T_N cells was prevented (Fig. 5*A*, *bottom panel*). $CD8^+$ T cell proliferation was reduced in the presence of blocking anti-class I mAb, whereas anti-class II mAb did not affect $CD8^+$ T cell proliferation (Fig. 5*A*, *bottom panel*). Myeloma-induced $CD8^+$ T cell proliferation produced DP-T cells, which accounted for 10–25%, and SP-$CD8^+$ T cells, which accounted for 68–83% of total $CD3^+$ T cells (Fig. 5*B*, *top panel*). Unlike their counterparts in myeloma-infiltrated bones, DP-T cells and SP-$CD8^+$ T cells derived in

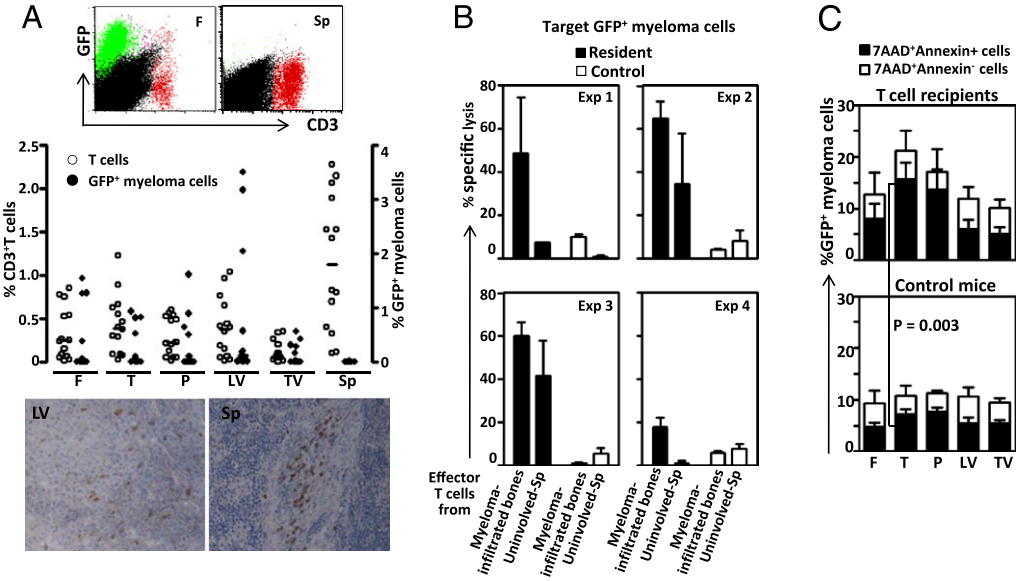

FIGURE 3. Alloreactive T cells with cytotoxic activity against resident myeloma cells arise in myeloma-infiltrated bones of T cell recipients. *A*, Flow cytometry analysis of the $CD3^+$ T cells and GFP^+ myeloma cells in the myeloma-infiltrated bones and uninvolved Sp of T cell recipients (dot plots, $CD3^+$ T cells depicted in red, GFP^+ myeloma cells in green). Individual data points represent the percentage of $CD3^+$ T cells (*left* y-*axis*) and GFP^+ myeloma cells (*right* y-*axis*) in myeloma-infiltrated bones and uninvolved Sp of the T cell recipients (at day 9–10 after T_N cell injection, scatter plot with median; $n = 14$). Immunohistochemistry staining of $CD3^+$ T cells in the lumbar vertebrae (LV) and Sp of T cell recipients (at day 7 after T_N cell injection, brown staining $CD3^+$ T cells, original magnifications ×20). *B*, Cytotoxic activity of allogeneic T cells from myeloma-infiltrated bones and uninvolved Sp of T cell recipients against the resident myeloma cells (harvested from myeloma-infiltrated bones of T cell recipients at day 9–10 after T_N cell injection, day 16–17 after the initial myeloma cell injection) and control myeloma cells (harvested from myeloma-infiltrated bones of control mice at day 16–17 after the initial myeloma cell injection). Results (bar, mean ± SEM) are from four representative [^{51}Cr] release experiments using E:T ratio 25:1, with similar results obtained using E:T ratio 50:1. *C*, Proportions of late apoptotic (7-AAD^+ annexin V^+) and necrotic (7-AAD^+ annexin V^- cells) myeloma cells in the myeloma-infiltrated bones and uninvolved Sp of T cell recipients and control mice (at day 9–10 after T_N cell injection, day 16–17 after the initial myeloma cell injection; bar, mean ± SEM; 4–5 mice/group).

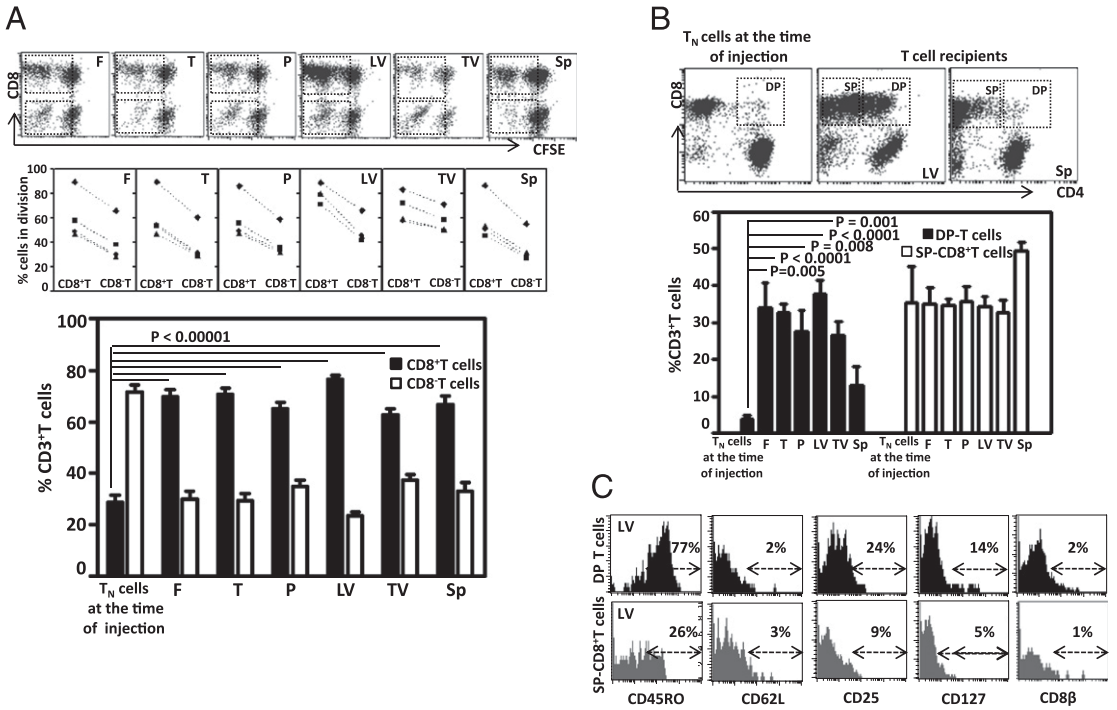

FIGURE 4. Proliferation and differentiation of adoptively transferred T_N cells in T cell recipients. *A*, The $CD8^+$ T and $CD8^-$ T cell proliferation defined by the CFSE division-tracking assay in myeloma-infiltrated bones and uninvolved Sp of the T cell recipients (at day 7 after T_N cell injection). *Top panel*, Dividing $CD8^+$ T and $CD8^-$ T cells in dot plots outlined by squares. *Middle panel*, Symbols represent the percentage of dividing $CD8^+$ T and $CD8^-$ T cells in myeloma-infiltrated bones and uninvolved Sp of individual T cell recipients; paired $CD8^+$ T and $CD8^-$ T cells from individual mice are connected. *Bottom panel*, Percentage of $CD8^+$ T and $CD8^-$ T cells among T_N cells at the time of injection and in myeloma-infiltrated bones and uninvolved Sp of the T cell recipients (bar, mean ± SEM, $n = 9$). *B*, Flow cytometry analysis of DP-T cells and SP-$CD8^+$ T cells among T_N cells at the time of injection and in myeloma-infiltrated lumbar vertebrae (LV) and uninvolved Sp of the T cell recipients (dot plots; bar, mean ± SEM, $n = 9$). *C*, Histograms show expression of the indicated Ag on DP-T cells and SP-$CD8^+$ T cells in the LV (representative of DP-T cells and SP-$CD8^+$ T cells in other myeloma-infiltrated bones) of T cell recipients. Percentages represent the proportion of cells that stained positive for indicated Ag (arrow, gate defining Ag positivity above background level defined on unstained cells).

coculture with myeloma cells resembled the phenotype of T central memory (T_{CM}) cells expressing CD45RO, CD62L, CD127, and CD25 surface Ags. DP-T cells and SP-$CD8^+$ T cells derived in coculture with myeloma cells maintained higher levels of CD8β compared with their counterparts in myeloma-infiltrated bones (Fig. 5*B*, *middle panel*). Consistent with their T_{CM} phenotype, DP-T cells and SP-$CD8^+$ T cells derived in coculture with myeloma cells produced perforin, but not IFN-γ (Fig. 5*B*, *bottom panel*). These data suggest a critical role for myeloma cells in the priming of alloreactive T cells in a class I-dependent manner. They also indicate that myeloma-induced alloreactive T cells produced via in vitro cultures, unlike those arising in myeloma-infiltrated bones, fail to acquire a phenotype resembling T_{EM} cells.

DP-T cells and SP-T cells arising in myeloma-infiltrated bones produce and secrete cytotoxic mediators

Observations that DP-T cells and SP-$CD8^+$ T cells arising in myeloma-infiltrated bones display a phenotype resembling T_{EM} cells and exert cytotoxic activity against resident myeloma suggest that they should be able to produce and secrete cytotoxic mediators such as IFN-γ or perforin. Indeed, 40–53% of DP-T cells expressed either IFN-γ or perforin or coexpressed both IFN-γ and perforin and comprised fewer T_{CM} cells (IFN-γ^- perforin$^-$ cells) compared with SP-$CD8^+$ T cells (Fig. 6*A*). In contrast to previous studies that suggest that DP-T cells obtained from breast and melanoma cancer are able to produce IL-5 and IL-13 (16, 17), in our study DP-T cells and SP-$CD8^+$ T cells arising in the myeloma-infiltrated bones did not express IL-5, IL-13, or IL-2 (data not shown). Both DP-T cells and SP-$CD8^+$ T cells arising in the myeloma-infiltrated bones included degranulated $CD107a^+$ T cells, indicative of their ability to secrete perforin (18, 19). SP-$CD8^+$ T cells in myeloma-infiltrated bones appeared to be more prone to degranulation and perforin secretion because they included more degranulated $CD107a^+$ T cells than SP-$CD8^+$ T cells from uninvolved Sp (Fig. 6*B*). Enrichment of degranulated $CD107a^+$ T cells in myeloma-infiltrated bones was consistent with higher levels of perforin seen in myeloma-infiltrated femur and tibia than in the uninvolved Sp of T cell recipients (Fig. 6*C*). Overall, these data suggest that DP-T cells and SP-$CD8^+$ T cells in myeloma-infiltrated bones are stimulated to produce and secrete cytotoxic mediators to fuel their cytotoxic antimyeloma activity.

Discussion

Defining the type of effector T cells and the cellular mechanisms involved in myeloma elimination by alloreactive T cells remains a key challenge for improvement of GVM responses in allotransplanted MM recipients. In this study, using adoptive transfer of T_N cells into myeloma-bearing mice, we provide evidence that myeloma cells are able to induce alloreactive T cells in the myeloma-infiltrated bones of T cell recipients. These myeloma-induced alloreactive T cells eliminate resident myeloma, leading to transient myeloma suppression and prolonged survival of T cell recipient mice. Myeloma-induced alloreactive T cells include nonconventional DP-T ($CD8\alpha\alpha^+CD4^+$) cells that produce and secrete cytotoxic mediators, IFN-γ and perforin, and therefore are likely to be involved in the GVM effect.

We found that priming of alloreactive T cells by RPMI8226-TGL myeloma cells was MHC class I restricted because priming was

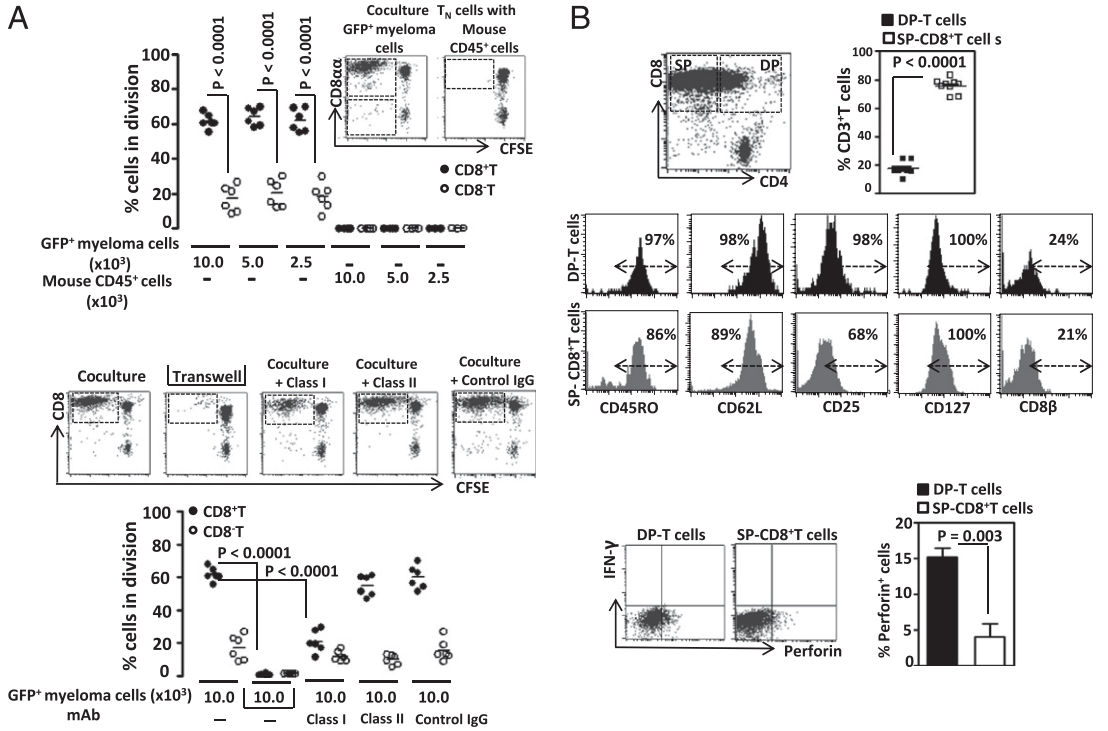

FIGURE 5. Myeloma cells prime alloreactive T cells in MHC class I and contact-dependent fashion and induce DP-T cells. Myeloma cells or mouse $CD45^+$ cells sorted from the same myeloma-infiltrated bones of individual myeloma-bearing mice (day 30–35 after the myeloma cell injection) were cultured with T_N cells (1×10^5 $CD3^+CD45RA^+$ cells; from two healthy donors) in coculture or Transwell assay. *A*, The proliferation of $CD8^+$ T and $CD8^-$ T cells was defined by the CFSE division-tracking assay at day 5 of culture in coculture assay without or with blocking anti-class I, anti-class II, or control IgG mAb or Transwell assay (representative dot plots, dividing $CD8^+$ T and $CD8^-$ T cells outlined by squares; scatter plot with mean, $n = 6$). *B*, Flow cytometric analysis of DP-T cells and SP-$CD8^+$ T cells derived in the coculture assay with myeloma cells (10×10^3 GFP^+ myeloma cells; dot plots; scatter plot with mean, $n = 9$). Histograms show expression of the indicated Ag on DP-T cells and SP-$CD8^+$ T cells (percentages represent the proportion of cells that stained positive for indicated Ag; arrow, gate defining Ag positivity above background level defined on unstained cells). Flow cytometric analysis of IFN-γ and perforin in DP-T cells and SP-$CD8^+$ T cells derived in the coculture assay with myeloma cells (10×10^3 GFP^+ myeloma cells; dot plots; bar, mean ± SEM, $n = 5$).

blocked in the presence of W6/32, a pan MHC class I mAb. Thus, RPMI8226-TGL myeloma cells mirror the Ag-presenting capacity of $CD38^+$ plasma cells obtained from bone marrow aspirates of MM patients (20) and are able to present peptide in the context of self MHC class I molecule to alloreactive T cells. This implies that in transplanted MM recipients, MHC class I molecule expression by malignant plasma cells and contact between plasma cells and transplanted T cells in myeloma-involved bones may be two important parameters determining the development of alloreactive T cell responses and the GVM effect.

One intriguing observation in our study is that myeloma-induced alloreactive T cells exert cytotoxic activity against resident myeloma cells obtained from T cell recipient mice, but not against control myeloma cells obtained from myeloma-bearing mice that did not receive T_N cells. Due to the lack of MM cell lines and nonmyeloma cells that are HLA matched with RPMI8226-TGL (21), it was not possible to determine whether the peptide recognized by the alloreactive T cells on resident RPMI8226-TGL myeloma cells was shared with other MM cell lines or nonmyeloma cells. How alloreactive T cells discriminate between resident myeloma cells and control myeloma cells is unclear. It is possible that in the course of immunosurveillance by alloreactive T cells, myeloma cells undergo immune transformation, as part of immunoediting process (22), which may enhance their immune recognition by alloreactive T cells. In T cell recipients, components of the MHC class I processing and presentation pathway may be changed by IFN-γ (23) produced by alloreactive T cells, and these changes may select alloreactive T cells that discriminate between resident myeloma cells and control myeloma cells. It is conceivable that these selected alloreactive T cells can also lead to myeloma-Ag–specific recognition. Further work in defining allorestricted myeloma-Ag–specific T cells in preclinical myeloma-bearing mouse models has important implications for current DLI treatment. In clinical settings, infusion of allorestricted T cells with known specificity for myeloma Ag, as opposed to infusion of whole donor lymphocytes, could generate a specific GVM effect.

DP-T cells are generally found in the thymus as immature thymocytes that during maturation lose either CD4 or CD8 coreceptors and emigrate to the periphery as mature SP-$CD4^+$ T and SP-CD8αβ cells (24). Our study demonstrates that myeloma stimulation leads to an accumulation of DP-T cells in myeloma-infiltrated bones, a target organ for MM, but not in uninvolved Sp. This extends data from several other studies, suggesting that DP-T cells are accumulated in target organs of various diseases, such as the thyroid gland in patients with autoimmune thyroiditis (25), the skin of patients with atopic dermatitis and systemic sclerosis (26, 27), and the joint fluid of patients with rheumatoid arthritis (28). In addition, DP-T cells have been reported in patients with cancer (16, 17, 29) and infectious diseases (30, 31), and in allogeneic hematopoietic stem cell transplant recipients (32). The vast majority of DP-T cells arising in myeloma-infiltrated bones converted CD8αβ heterodimer (expressed on SP-$CD8^+$ T_N prior to adoptive transfer into myeloma-bearing mice) to CD8αα homodimer. This phenotype makes the DP-T cells present in myeloma-infiltrated bones similar to DP-T cells found in Hodgkin's

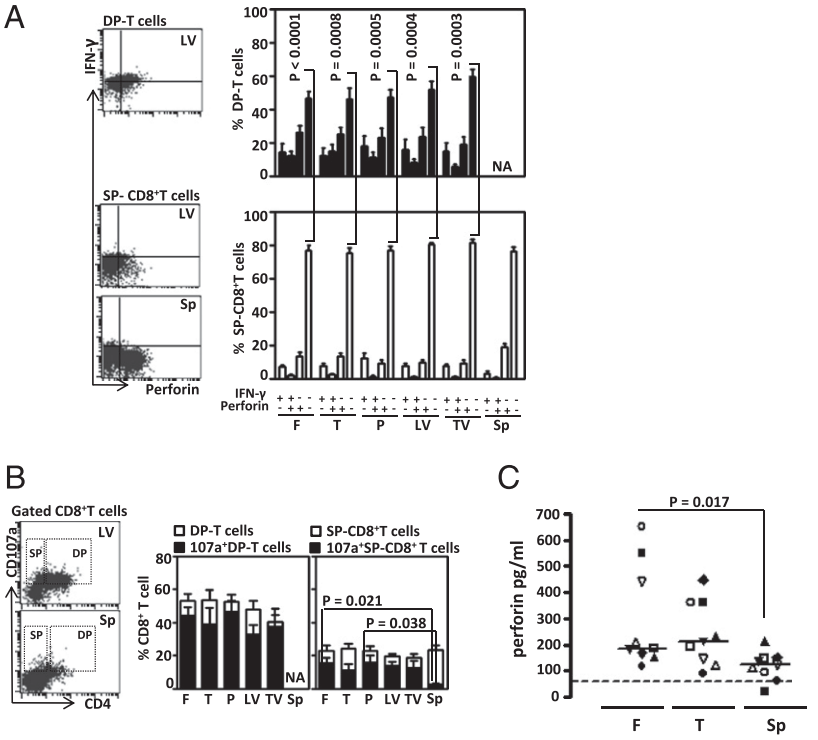

FIGURE 6. DP-T cells and SP-T cells arising in myeloma-infiltrated bones produce and secrete cytotoxic mediators. *A*, Flow cytometry analysis of IFN-γ and perforin in DP-T cells and SP-CD8$^+$ T cells in myeloma-infiltrated bones and uninvolved Sp of the T cell recipients (at day 9–10 after T_N cell injection, dot plots; bar, mean ± SEM, $n = 7$; NA, not analyzed due to the paucity of DP-T cells in uninvolved Sp). *B*, Flow cytometry analysis of CD107a expression on DP-T cells and SP-CD8$^+$ T cells in myeloma-infiltrated bones and uninvolved Sp of the T cell recipients (at day 9–10 after T cell injection, dot plots; bar, mean ± SEM, $n = 9$). *C*, Perforin concentration detected in the myeloma-infiltrated F and T and uninvolved Sp of individual T cell recipients (at day 9–10 after T_N cell injection, day 14–15 after initial myeloma cell injection; symbols identify individual T cell recipients, scatter plot with median, $n = 9$). Dotted line represents the lowest detectable standard perforin concentration (0.062 μg/ml) above background level.

lymphoma (29), Kawasaki's disease (33), and inflammatory bowel disease (34), but discriminates them from DP-T cells found in breast cancer and melanoma that express the CDαβ heterodimer (16, 17). Functional studies on tumor-associated DP-T cells expressing CD8αβ heterodimer or CD8αα homodimer are still lacking, precluding understanding of the physiological relevance of each particular cell subset.

Although other studies suggest that DP-T can originate from SP-CD4$^+$ T cells (34, 35) or SP-CD8$^+$ T cells (36–40), our data suggest that myeloma-induced DP-T cells are generated through MHC class I molecule-dependent stimulation, and thus, are likely to originate from SP-CD8$^+$T cells. This observation adds myeloma cells to the growing list of stimuli, including superantigen (36), anti-CD3/CD28 Ab (37, 38), and allogeneic dendritic cells (39, 40) that can induce CD4 expression on SP-CD8$^+$ T cells. The mechanisms leading to CD4 expression on SP-CD8$^+$ T cells remain unclear; however, an early study suggested that it is mediated by silencing of the CD4 gene silencer (38). The appearance of DP-T cells in myeloma-infiltrated bones raises the question whether DP-T cells can be induced in uninvolved bone marrow by resident APCs.

Despite substantial evidence that DP-T cells are present in the tumor environment (16, 17, 29), evidence for their role in antitumor responses is minimal. To our knowledge, only one study has shown that DP-T cells infiltrating a cutaneous T cell lymphoma exert cytotoxic antitumor activity (41). In this study, we show that alloreactive DP-T cells present in myeloma-infiltrated bones possess important cytotoxic effector qualities, express IFN-γ, and degranulate and release perforin. Therefore, DP-T cells are likely to contribute to the overall cytotoxicity exerted by alloreactive T cells against resident myeloma cells.

It should be noted that DP-T cells are often produced through in vitro culture with polyclonal or Ag-specific stimuli (16, 17). These studies suggest that breast and melanoma cancer DP-T cells produced in in vitro culture are biased toward IL-5 and IL-13 production (16, 17). In our study, myeloma-induced DP-T cells in myeloma-infiltrated bones did not produce IL-5 and IL-13. Nonetheless, our data suggest that myeloma-induced DP-T cells produced through in vitro culture display a different phenotype and functional attributes compared with DP-T cells arising in myeloma-infiltrated bones. In vitro myeloma-induced DP-T cells retained CD62L, CD127, and upregulated CD25, and failed to express IFN-γ. In contrast, myeloma-induced DP-T cells arising in myeloma-infiltrated bones progressed to a more advanced differentiation stage characterized by lack of CD62L, CD25, and CD127, and almost half of them acquired the capacity to produce IFN-γ and/or perforin. From our experiments, it became clear that DP-T cells maintained in in vitro culture, at least with myeloma cells, fail to display some important effector functions relevant for their in vivo development within myeloma-infiltrated bones. Therefore, caution should be exercised in evaluating the physiological relevance of DP-T cells, based on the characteristics of in vitro generated DP-T cells.

In this study, we show that a single injection of T_N cells suppresses myeloma progression in T cell recipients for ~12 d, and thereafter, myeloma growth recurs. Myeloma growth recurs despite continued persistence of DP-T cells in the bones of T cell recipients until the end stage of disease (data not shown), suggesting that myeloma escapes the initially efficacious immunosurveillance mediated by alloreactive T cells. Demonstration that myeloma elimination is followed by myeloma escape provides additional evidence that myeloma immunoediting can occur in T cell recipients. Importantly, the transient myeloma suppression seen in T cell recipients mimics the transient GVM effect often seen after DLI therapy in MM patients (4). This observation validates the capacity of our experimental system to reflect the clinical manifestations of MM and its utility to study aspects of allogeneic immunotherapy in the myeloma setting. In our myeloma-bearing mice, mechanisms such as T cell tolerization (42), suppression of alloreactive T cells (43), or myeloma spread to the extramedullary space (44) may explain why myeloma fails to be eliminated by the alloreactive T cells. It is also possible that the number of donor T_N cells injected is a critical determinant for myeloma suppression and its subsequent escape; therefore,

different modalities of donor T_N cell treatment may improve myeloma eradication. Future work involving the testing of different donor T cell treatment modalities in myeloma-bearing experimental models will provide insights into the points at which alloreactive T cells could be rationally delivered to enhance the GVM effect and prevent myeloma relapse.

Our study provides a previously unappreciated conceptual framework for the role of myeloma-induced alloreactive T cells in myeloma suppression, but also in myeloma escape, and, therefore, provides a rationale for the myeloma-immunoediting hypothesis. Involvement of myeloma cells in alloreactive T cell priming also helps to explain the apparent paradox of how DLI can induce a sustained remission in MM recipients when the initial allogeneic stem cell transplantation could not. A possible scenario is that at the time of initial allogeneic stem cell transplantation, which is almost always given with concurrent immunosuppression, an insufficient number of myeloma cells is present to stimulate GVM responses. DLI is usually given without immunosuppression to MM patients relapsing after allogeneic stem cell transplantation. At this time, these patients have more myeloma cells compared with the time of the initial allogeneic stem cell transplantation. This increase in the number of myeloma cells at the time of DLI increases the likelihood of interaction between myeloma cells and donor T cells, thus triggering GVM responses. Our study provides a rationale for monitoring the number of myeloma cells in bone marrow prior to DLI therapy as a parameter to predict effective GVM responses in MM-transplanted recipients.

Acknowledgments

We thank Kristen Gibbons (Mater Research Support Centre, Brisbane, QLD, Australia) for excellent statistical assistance. We thank Michael McGuckin for comments and suggestions on the manuscript.

Disclosures

The authors have no financial conflicts of interest.

References

1. Lokhorst, H. M., A. Schattenberg, J. J. Cornelissen, M. H. van Oers, W. Fibbe, I. Russell, N. W. Donk, and L. F. Verdonck. 2000. Donor lymphocyte infusions for relapsed multiple myeloma after allogeneic stem-cell transplantation: predictive factors for response and long-term outcome. *J. Clin. Oncol.* 18: 3031–3037.
2. Tricot, G., D. H. Vesole, S. Jagannath, J. Hilton, N. Munshi, and B. Barlogie. 1996. Graft-versus-myeloma effect: proof of principle. *Blood* 87: 1196–1198.
3. Bertz, H., J. A. Burger, R. Kunzmann, R. Mertelsmann, and J. Finke. 1997. Adoptive immunotherapy for relapsed multiple myeloma after allogeneic bone marrow transplantation (BMT): evidence for a graft-versus-myeloma effect. *Leukemia* 11: 281–283.
4. van der Griend, R., L. F. Verdonck, E. J. Petersen, P. Veenhuizen, A. C. Bloem, and H. M. Lokhorst. 1999. Donor leukocyte infusions inducing remissions repeatedly in a patient with recurrent multiple myeloma after allogeneic bone marrow transplantation. *Bone Marrow Transplant.* 23: 195–197.
5. Rozemuller, H., E. van der Spek, L. H. Bogers-Boer, M. C. Zwart, V. Verweij, M. Emmelot, R. W. Groen, R. Spaapen, A. C. Bloem, H. M. Lokhorst, et al. 2008. A bioluminescence imaging based in vivo model for preclinical testing of novel cellular immunotherapy strategies to improve the graft-versus-myeloma effect. *Haematologica* 93: 1049–1057.
6. Reddy, P., Y. Maeda, C. Liu, O. I. Krijanovski, R. Korngold, and J. L. Ferrara. 2005. A crucial role for antigen-presenting cells and alloantigen expression in graft-versus-leukemia responses. *Nat. Med.* 11: 1244–1249.
7. Guinan, E. C., J. G. Gribben, V. A. Boussiotis, G. J. Freeman, and L. M. Nadler. 1994. Pivotal role of the B7:CD28 pathway in transplantation tolerance and tumor immunity. *Blood* 84: 3261–3282.
8. Kündig, T. M., M. F. Bachmann, C. DiPaolo, J. J. Simard, M. Battegay, H. Lother, A. Gessner, K. Kühlcke, P. S. Ohashi, H. Hengartner, et al. 1995. Fibroblasts as efficient antigen-presenting cells in lymphoid organs. *Science* 268: 1343–1347.
9. Feuerer, M., P. Beckhove, N. Garbi, Y. Mahnke, A. Limmer, M. Hommel, G. J. Hämmerling, B. Kyewski, A. Hamann, V. Umansky, and V. Schirrmacher. 2003. Bone marrow as a priming site for T-cell responses to blood-borne antigen. *Nat. Med.* 9: 1151–1157.
10. Feuerer, M., P. Beckhove, Y. Mahnke, M. Hommel, B. Kyewski, A. Hamann, V. Umansky, and V. Schirrmacher. 2004. Bone marrow microenvironment facilitating dendritic cell: CD4 T cell interactions and maintenance of CD4 memory. *Int. J. Oncol.* 25: 867–876.
11. Ponomarev, V., M. Doubrovin, I. Serganova, J. Vider, A. Shavrin, T. Beresten, A. Ivanova, L. Ageyeva, V. Tourkova, J. Balatoni, et al. 2004. A novel triple-modality reporter gene for whole-body fluorescent, bioluminescent, and nuclear noninvasive imaging. *Eur. J. Nucl. Med. Mol. Imaging* 31: 740–751.
12. Ely, S. A., and D. M. Knowles. 2002. Expression of CD56/neural cell adhesion molecule correlates with the presence of lytic bone lesions in multiple myeloma and distinguishes myeloma from monoclonal gammopathy of undetermined significance and lymphomas with plasmacytoid differentiation. *Am. J. Pathol.* 160: 1293–1299.
13. Rawstron, A., S. Barrans, D. Blythe, F. Davies, A. English, G. Pratt, A. Child, G. Morgan, and A. Jack. 1999. Distribution of myeloma plasma cells in peripheral blood and bone marrow correlates with CD56 expression. *Br. J. Haematol.* 104: 138–143.
14. Vuckovic, S., F. S. Abdul Wahid, A. Rice, M. Kato, D. Khalil, R. Rodwell, and D. N. Hart. 2008. Compartmentalization of allogeneic T-cell responses in the bone marrow and spleen of humanized NOD/SCID mice containing activated human resident myeloid dendritic cells. *Exp. Hematol.* 36: 1496–1506.
15. Mitsiades, C. S., N. S. Mitsiades, R. T. Bronson, D. Chauhan, N. Munshi, S. P. Treon, C. A. Maxwell, L. Pilarski, T. Hideshima, R. M. Hoffman, and K. C. Anderson. 2003. Fluorescence imaging of multiple myeloma cells in a clinically relevant SCID/NOD in vivo model: biologic and clinical implications. *Cancer Res.* 63: 6689–6696.
16. Desfrançois, J., L. Derré, M. Corvaisier, B. Le Mével, V. Catros, F. Jotereau, and N. Gervois. 2009. Increased frequency of nonconventional double positive CD4CD8 alphabeta T cells in human breast pleural effusions. *Int. J. Cancer* 125: 374–380.
17. Desfrançois, J., A. Moreau-Aubry, V. Vignard, Y. Godet, A. Khammari, B. Dréno, F. Jotereau, and N. Gervois. 2010. Double positive CD4CD8 alphabeta T cells: a new tumor-reactive population in human melanomas. *PLoS One* 5: e8437.
18. Betts, M. R., J. M. Brenchley, D. A. Price, S. C. De Rosa, D. C. Douek, M. Roederer, and R. A. Koup. 2003. Sensitive and viable identification of antigen-specific CD8+ T cells by a flow cytometric assay for degranulation. *J. Immunol. Methods* 281: 65–78.
19. Hersperger, A. R., G. Makedonas, and M. R. Betts. 2008. Flow cytometric detection of perforin upregulation in human CD8 T cells. *Cytometry A* 73: 1050–1057.
20. Yi, Q., S. Dabadghao, A. Osterborg, S. Bergenbrant, and G. Holm. 1997. Myeloma bone marrow plasma cells: evidence for their capacity as antigen-presenting cells. *Blood* 90: 1960–1967.
21. Pellat-Deceunynck, C., G. Jego, J. L. Harousseau, H. Vié, and R. Bataille. 1999. Isolation of human lymphocyte antigens class I-restricted cytotoxic T lymphocytes against autologous myeloma cells. *Clin. Cancer Res.* 5: 705–709.
22. Dunn, G. P., L. J. Old, and R. D. Schreiber. 2004. The immunobiology of cancer immunosurveillance and immunoediting. *Immunity* 21: 137–148.
23. Kaplan, D. H., V. Shankaran, A. S. Dighe, E. Stockert, M. Aguet, L. J. Old, and R. D. Schreiber. 1998. Demonstration of an interferon gamma-dependent tumor surveillance system in immunocompetent mice. *Proc. Natl. Acad. Sci. USA* 95: 7556–7561.
24. Germain, R. N. 2002. T-cell development and the CD4-CD8 lineage decision. *Nat. Rev. Immunol.* 2: 309–322.
25. Iwatani, Y., Y. Hidaka, F. Matsuzuka, K. Kuma, and N. Amino. 1993. Intrathyroidal lymphocyte subsets, including unusual CD4+ CD8+ cells and CD3loTCR alpha beta lo/−CD4−CD8− cells, in autoimmune thyroid disease. *Clin. Exp. Immunol.* 93: 430–436.
26. Bang, K., M. Lund, K. Wu, S. C. Mogensen, and K. Thestrup-Pedersen. 2001. CD4+ CD8+ (thymocyte-like) T lymphocytes present in blood and skin from patients with atopic dermatitis suggest immune dysregulation. *Br. J. Dermatol.* 144: 1140–1147.
27. Chizzolini, C., Y. Parel, C. De Luca, A. Tyndall, A. Akesson, A. Scheja, and J. M. Dayer. 2003. Systemic sclerosis Th2 cells inhibit collagen production by dermal fibroblasts via membrane-associated tumor necrosis factor alpha. *Arthritis Rheum.* 48: 2593–2604.
28. De Maria, A., M. Malnati, A. Moretta, D. Pende, C. Bottino, G. Casorati, F. Cottafava, G. Melioli, M. C. Mingari, N. Migone, et al. 1987. CD3+4−8−WT31−(T cell receptor gamma+) cells and other unusual phenotypes are frequently detected among spontaneously interleukin 2-responsive T lymphocytes present in the joint fluid in juvenile rheumatoid arthritis: a clonal analysis. *Eur. J. Immunol.* 17: 1815–1819.
29. Rahemtullah, A., K. K. Reichard, F. I. Preffer, N. L. Harris, and R. P. Hasserjian. 2006. A double-positive CD4+CD8+ T-cell population is commonly found in nodular lymphocyte predominant Hodgkin lymphoma. *Am. J. Clin. Pathol.* 126: 805–814.
30. Weiss, L., A. Roux, S. Garcia, C. Demouchy, N. Haeffner-Cavaillon, M. D. Kazatchkine, and M. L. Gougeon. 1998. Persistent expansion, in a human immunodeficiency virus-infected person, of V beta-restricted CD4+CD8+ T lymphocytes that express cytotoxicity-associated molecules and are committed to produce interferon-gamma and tumor necrosis factor-alpha. *J. Infect. Dis.* 178: 1158–1162.
31. Ortolani, C., E. Forti, E. Radin, R. Cibin, and A. Cossarizza. 1993. Cytofluorimetric identification of two populations of double positive (CD4+,CD8+) T lymphocytes in human peripheral blood. *Biochem. Biophys. Res. Commun.* 191: 601–609.
32. Storek, J., M. A. Dawson, B. Storer, T. Stevens-Ayers, D. G. Maloney, K. A. Marr, R. P. Witherspoon, W. Bensinger, M. E. Flowers, P. Martin, et al.

2001. Immune reconstitution after allogeneic marrow transplantation compared with blood stem cell transplantation. *Blood* 97: 3380–3389.
33. Hirao, J., and K. Sugita. 1998. Circulating CD4+CD8+ T lymphocytes in patients with Kawasaki disease. *Clin. Exp. Immunol.* 111: 397–401.
34. Das, G., M. M. Augustine, J. Das, K. Bottomly, P. Ray, and A. Ray. 2003. An important regulatory role for CD4+CD8 alpha alpha T cells in the intestinal epithelial layer in the prevention of inflammatory bowel disease. *Proc. Natl. Acad. Sci. USA* 100: 5324–5329.
35. Paliard, X., R. W. Malefijt, J. E. de Vries, and H. Spits. 1988. Interleukin-4 mediates CD8 induction on human CD4+ T-cell clones. *Nature* 335: 642–644.
36. Sullivan, Y. B., A. L. Landay, J. A. Zack, S. G. Kitchen, and L. Al-Harthi. 2001. Upregulation of CD4 on CD8+ T cells: CD4dimCD8bright T cells constitute an activated phenotype of CD8+ T cells. *Immunology* 103: 270–280.
37. Laux, I., A. Khoshnan, C. Tindell, D. Bae, X. Zhu, C. H. June, R. B. Effros, and A. Nel. 2000. Response differences between human CD4(+) and CD8(+) T-cells during CD28 costimulation: implications for immune cell-based therapies and studies related to the expansion of double-positive T-cells during aging. *Clin. Immunol.* 96: 187–197.
38. Flamand, L., R. W. Crowley, P. Lusso, S. Colombini-Hatch, D. M. Margolis, and R. C. Gallo. 1998. Activation of CD8+ T lymphocytes through the T cell receptor turns on CD4 gene expression: implications for HIV pathogenesis. *Proc. Natl. Acad. Sci. USA* 95: 3111–3116.
39. Kitchen, S. G., Y. D. Korin, M. D. Roth, A. Landay, and J. A. Zack. 1998. Costimulation of naive CD8(+) lymphocytes induces CD4 expression and allows human immunodeficiency virus type 1 infection. *J. Virol.* 72: 9054–9060.
40. Yang, L. P., J. L. Riley, R. G. Carroll, C. H. June, J. Hoxie, B. K. Patterson, Y. Ohshima, R. J. Hodes, and G. Delespesse. 1998. Productive infection of neonatal CD8+ T lymphocytes by HIV-1. *J. Exp. Med.* 187: 1139–1144.
41. Bagot, M., H. Echchakir, F. Mami-Chouaib, M. H. Delfau-Larue, D. Charue, A. Bernheim, S. Chouaib, L. Boumsell, and A. Bensussan. 1998. Isolation of tumor-specific cytotoxic CD4+ and CD4+CD8dim+ T-cell clones infiltrating a cutaneous T-cell lymphoma. *Blood* 91: 4331–4341.
42. Shankaran, V., H. Ikeda, A. T. Bruce, J. M. White, P. E. Swanson, L. J. Old, and R. D. Schreiber. 2001. IFNgamma and lymphocytes prevent primary tumour development and shape tumour immunogenicity. *Nature* 410: 1107–1111.
43. Atanackovic, D., Y. Cao, T. Luetkens, J. Panse, C. Faltz, J. Arfsten, K. Bartels, C. Wolschke, T. Eiermann, A. R. Zander, et al. 2008. CD4+CD25+FOXP3+ T regulatory cells reconstitute and accumulate in the bone marrow of patients with multiple myeloma following allogeneic stem cell transplantation. *Haematologica* 93: 423–430.
44. Zeiser, R., B. Deschler, H. Bertz, J. Finke, and M. Engelhardt. 2004. Extramedullary vs medullary relapse after autologous or allogeneic hematopoietic stem cell transplantation (HSCT) in multiple myeloma (MM) and its correlation to clinical outcome. *Bone Marrow Transplant.* 34: 1057–1065.